Available online at www.sciencedirect.com
SCIENCE DIRECT®
Cancer Letters 228 (2005) 71–81
CANCER Letters
www.elsevier.com/locate/canlet

Mini-review

High-resolution cDNA microarray-based comparative genomic hybridization analysis in neuroblastoma

Qing-Rong Chen[1], Sven Bilke[1], Javed Khan*

Oncogenomics Section, Pediatric Oncology Branch, Advanced Technology Center, National Cancer Institute, 8717 Government Circle, Gaithersburg, MD 20877, USA

Received 24 November 2004; accepted 14 December 2004

Abstract

Neuroblastoma (NB) is one of the most common pediatric solid tumors and displays a broad variety of genomic alterations. Array-based comparative genomic hybridization (A-CGH) is a novel technology enabling the high-resolution detection of DNA copy number aberrations. In this article, we outline features of this new technology and approaches of data analysis. We focus on stage specific DNA copy number variations in neuroblastoma detected by cDNA array-based comparative genomic hybridization (A-CGH). We also discuss hypothetic evolutionary models of neuroblastoma progression that can be derived from A-CGH data.
Published by Elsevier Ireland Ltd.

Keywords: Neuroblastoma; Array CGH; Microarray; Tumor evolution; DNA copy number; Genomic alteration; Amplification; *MYCN*

1. Introduction

Neuroblastoma (NB) is a tumor derived from primitive cells of the sympathetic nervous system and is one of the most common pediatric solid tumors. The disease is characterized by diverse clinical behaviors ranging from spontaneous regression to rapid malignant progression [1]. Many important factors such as stage, age and ploidy have been identified to be associated with the biological and clinical heterogeneity of NB tumors. This diverse biological behavior makes NB a paradigm for the investigation of genomic alterations and associating it with clinical outcome. In neuroblastoma, genomic alterations have been investigated by cytogenetic, and molecular methods including spectral karyotyping and metaphase comparative genomic hybridization (M-CGH) [2–6]. Here, we focus on DNA copy number alterations in NB detected by the recently developed cDNA array-based comparative genomic hybridization (A-CGH). This review will describe and illustrate this new technology and its application in NB, and will discuss novel analysis approaches currently used in DNA array CGH profiling that reduces noise and increases sensitivity to detect genomic alterations at high resolution.

* Corresponding author. Tel.: +1 301 435 2937; fax: +1 301 480 0314/402 3134.
E-mail addresses: chenqi@mail.nih.gov (Q.-R. Chen), bilkes@mail.nih.gov (S. Bilke), khanjav@mail.nih.gov (J. Khan).
[1] Qing-Rong Chen and Sven Bilke: Equal contributor.

0304-3835/$ - see front matter Published by Elsevier Ireland Ltd.
doi:10.1016/j.canlet.2004.12.056

2. Array-CGH

Comparative genomic hybridization (CGH) was developed as a molecular cytogenetic technique to compensate for the difficulties presented by conventional cytogenetics and fluorescence in situ hybridization (FISH) analysis; it does not require culturing of tumor cells in vitro and has substantially increased genome-wide information on unbalanced chromosomal changes [7]. Many novel and non-random genomic alterations in NB have been detected using metaphase CGH (M-CGH) analyses [3,8,9], however, this technique is hampered by a limited resolution of 10–20 Mb. To overcome this, array-based CGH (A-CGH) on BAC, cDNA or oligonucleotides microarray has been developed and can detect genomic alterations with higher resolution [10–15] which is determined by the distribution and spacing of the clones along the genome. Relative copy number is measured at these specific loci by hybridization of fluorescently labeled test and reference DNA as in conventional M-CGH [11,13]. Since, the clones used on the array contain sequence tags, their positions are accurately known relative to the genome sequence, and genes mapping within regions of copy number alteration can be readily identified. Arrays comprised of large insert genomic clones such as BACs provide reliable copy number measurements on individual clones, since they generally have a higher signal to noise ratio. Both small and large DNA arrays have been made consisting of ~2500 BAC clones represent at an average interval of ~1.4 Mb [12] to large tiling-array of 32,433 overlapping BAC clones covering the entire genome [16]. The latter increases the ability of BAC A-CGH to identify genetic alterations and their boundaries throughout the genome in much higher resolution. The limitations of BAC A-CGH, include the fact that preparation and spotting of BAC DNA is labor intensive and can be very expensive [17], and that each clone may represent more than one gene and it is not possible to do parallel gene expression and copy number changes using the same arrays.

A-CGH on cDNA arrays have the distinct advantage of providing a direct method to detect individual gene copy number changes in unbalanced chromosomal rearrangements [13]. The second significant advantage is that it allows us to investigate the direct effects of genomic changes over gene expression level by using the same microarray for both ACGH and gene expression analysis [18,19]. However, because of lower signal to noise ratios the detection of lower copy number changes requires additional methods such as calculating the running average of multiple clones along the genome, where typically 5–10 clones are used. It is also frequently necessary to discard measurements on a substantial fraction of clones because they do not provide adequate signals. Thus, the actual genomic resolution of the boundaries of single copy changes and the ability to detect focal single copy changes is considerably less than implied by the average genomic spacing between the clones on the array.

More recently, oligonucleotide-based arrays have been used for DNA copy number analysis [20–22]. The studies clearly showed the ability to detect high-level amplifications and to determine the boundaries of high copy number portions of the genome. Single copy changes could be detected in different resolutions depending on the type of oligo-arrays and the techniques of hybridization. However, like with cDNA arrays, detection of single copy changes requires running average with a corresponding reduction in genomic resolution. Oligo-based microarrays hold the potential of enhanced design flexibility and full-genome representation of probes capable of accurately reporting single-copy number changes.

3. Amplicon mapping by cDNA array CGH in NB

Conventional CGH profiling of NBs has identified many genomic aberrations, although the limited resolution has precluded a precise localization of sequences of interest within amplicons. Application of cDNA A-CGH in NB allows genome-wide identification of amplified genes [14,23,24]. In a recent study, we performed A-CGH for 12 NB cell lines and 32 NB primary tumor samples using microarrays containing 42,000 cDNA clones (~24,000 UniGenes) [14]. We found that only two chromosomes (2p and 12q) showed amplifications and all in the *MYCN* amplified samples (Fig. 1A and B). Focusing on 2p (Fig. 1A), we found six independent non-contiguous amplicons (10.4–69.4 Mb). For the *MYCN* amplicon, the largest contiguous region was 1.7 Mb and bounded by *NAG*

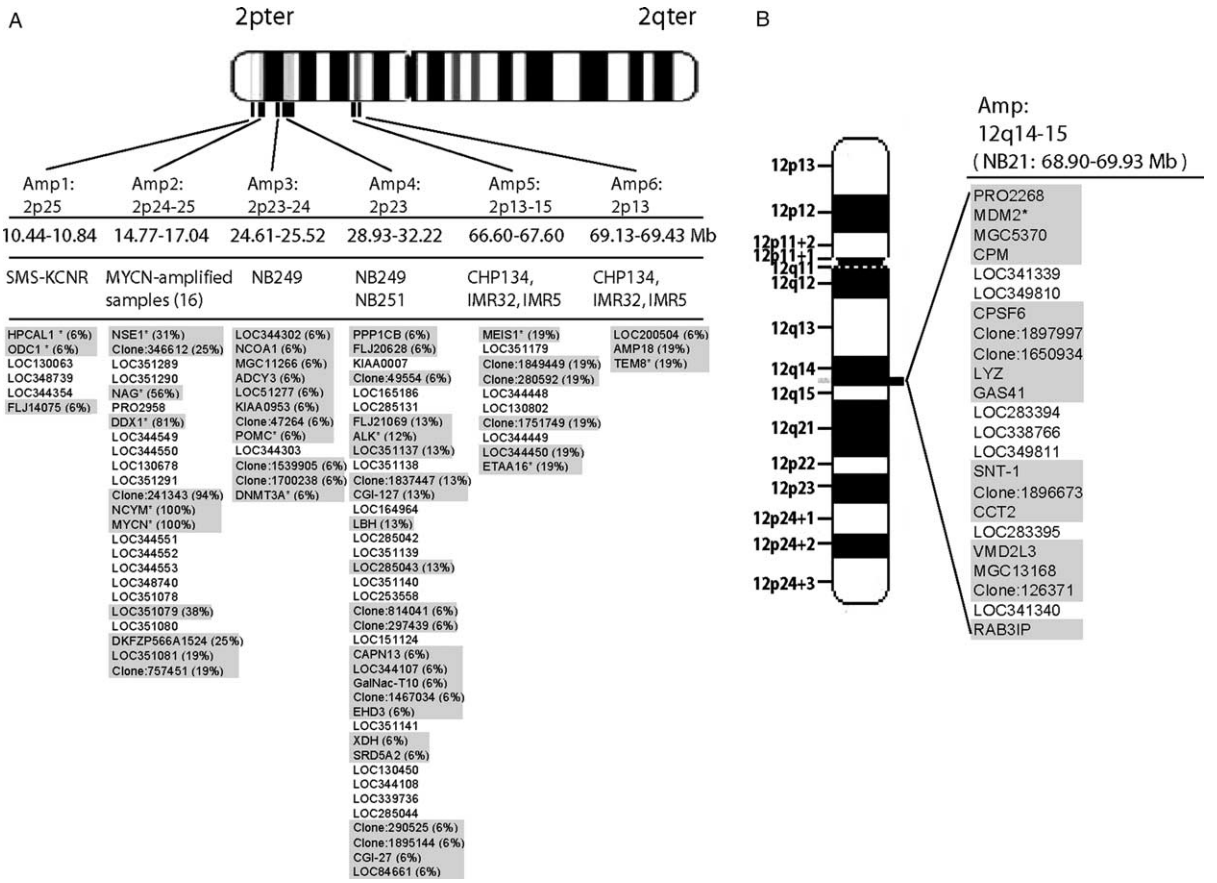

Fig. 1. Amplifications in *MYCN* amplified samples. (A) Independent amplicons in chromosome 2p. All amplified genes are listed under each amplicon in genome order. Map position, genome sequence position (Mb) and samples containing the specific amplicon are listed for each amplicon. The percentage of the *MYCN* amplified samples harboring these amplicons are shown in brackets following the gene name for all clones present in our microarray (gray), the remainder of the clones are predicted genes found in the NCBI database that are mapped between the boundaries of the amplicon. (B) Amplicon in chromosome 12q in tumor NB21. Figure taken from [14] and used with permission.

and an EST (clone: 757451), whilst the smallest region was 27 kb including an EST (clone: 241343), *NCYM*, and *MYCN*. We identified nine previously reported co-amplified genes (*HPCAL1*, *ODC1*, *NSE1*, *NAG*, *DDX1*, *NCYM*, *POMC*, *DNMT3A*, *ALK*, *MEIS1*, *TEM8*) [23–31], and detected the novel amplification of several known genes (*NCOA1*, *ADCY3*, *PPP1CB*, *CGI-127*, *LBH*, *CAPN13*, *GalNac-T10*, *EHD3*, *XDH*, *SRD5A2*, *CGI-27*, *AMP18*) and ESTs. Three of the cell lines (CHP134, IMR-5 and IMR-32) contained two amplicons in 2p13-15. The first (66.6–67.6 Mb) included previously reported amplified gene *MEIS1*, and the size of the second amplicon was 0.3 Mb (69.1–69.4 Mb), which was bounded by *LOC200504* and *TEM8*. In addition to chromosome 2p, we identified another amplicon on 12q14-q15 in a *MYCN* amplified tumor; bounded by *PRO2268* (68.9 Mb) and *RAB3IP* (69.9 Mb) containing one previously reported amplified gene (*MDM2*) [32] as well as several novel amplifications (*CPM*, *CPSF6*, *LYZ*, *GAS41*, *SNT-1*, *CCT2*, *VMD2L3*, and *RAB3IP*) (Fig. 1B).

4. Probabilistic analysis of cDNA A-CGH profile

It has been reported that BAC A-CGH is more sensitive than cDNA or oligonucleotide A-CGH in detecting genomic alterations because of the long

sequence of BAC clones and higher signal to noise ratios. The majority of the reported applications of cDNA or oligonucleotide based A-CGH has focused on amplifications [23,24], where typically more than 10 extra copies of DNA are gained. However, low-level DNA gains and losses are difficult to detect for the cDNA or oligonucleotide-based A-CGH due to a lower signal to noise ratio. To increase the sensitivities for lower level DNA copy number changes, a 'running average' smoothing filter has been used as a noise reduction strategy [18,19]. Using running average of multiple clones typically 5–10 along the genome, the actual genomic resolution of the boundaries of changes and the ability to detect focal copy number changes is considerably less than implied by the average genomic spacing between the clones on the array.

We analyzed both theoretically and experimentally the performances of the running average smoothing filter for cDNA A-CGH data and found the noise reduction performance of running average was much lower than expected due in large part to systematic errors in the data [15]. In our theoretical analysis, we derived an equation, which linked the sensitivity (the lowest detectable level of copy number changes) with the size of the window used in the running average procedure. The analytic calculations demonstrate that with a window size 10 it is possible to safely detect gains of three extra copies in diploid cells. Larger window sizes are necessary in order to detect losses with sufficient statistical certainty. The application of the running average algorithm is based on several assumptions. Some of those assumptions are not met, more specifically that the noise is randomly distributed and that the variance is approximately constant on the whole genome. We thus developed a novel algorithm, topological statistics (TS), to reduce this type of errors [15]. The reduction of statistical noise is performed by combining measurements within a sliding window into one estimator like running average. The difference to the running average is that this estimator is then compared to a null-distribution representing the unchanged DNA configuration. The algorithm is based on comparison of the biological relevant data to data from self–self hybridizations, which contain no biological information but contain systematic errors. The systematic errors are canceled out by comparing the window content to observations of this neutral dataset (self–self hybridizations) assuming that they approximately carry the same systematic errors. The effectiveness of TS strongly depends on this assumption; the best results were obtained when the self–self hybridizations used in the analysis were generated under similar conditions using the same print-batch. This algorithm provides a probabilistic estimate for the presence of genomic alterations and assigns a *P*-value to the center of the sliding window. We used *t*-test for the comparison of the two distributions, but the method is not limited to this statistics. Fig. 2 showed the heatmap of the raw ratio data, the same data smoothened with running average (RA) and topological statistics (TS) for four neuroblastoma cell lines. Recently, two other algorithms were reported for the analysis of CGH data, mainly focusing on an automatized detection of breakpoints [33,34]. One reported the good performance of their algorithm for signal to noise ratio larger than $\sim$2.5 [33]. Another one has no estimate for the effective resolution and sensitivity of the algorithm [34].

5. Detection of low-level DNA copy number alterations by cDNA A-CGH in NB

There are several studies using cDNA A-CGH to detect the amplification in NB [14,23,24], however, not many have used the technique to identify low-level genomic alterations in NB. In order to increase the sensitivity for detecting low copy number changes, we applied the probabilistic approach (topological statistics discussed above) utilizing statistics and the local genomic sequence mapping information of each of the cDNA clones on our arrays [14,15]. We validated the method by analyzing the A-CGH data generated from the cell lines containing 1–5 copies of the X chromosome and were able to detect a single copy loss and gain of X chromosome, where the expected ratio was 0.5 and 1.5, respectively. As an independent validation of our method, albeit at lower resolution, we performed standard metaphase CGH (M-CGH) on one NB cell line (GILIN) in parallel. Our results demonstrated good genome-wide concordance for losses and gains detected by both A-CGH and M-CGH (Fig. 3). In addition, we used the reported results from the literature as an independent

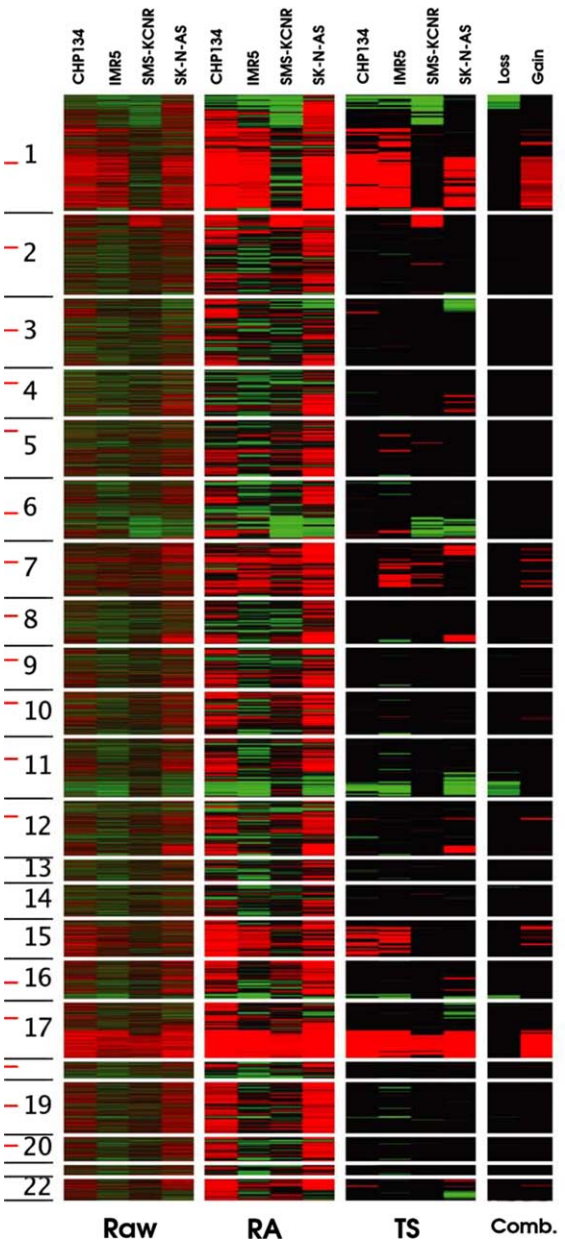

Fig. 2. Comparison of different A-CGH data analysis approaches. Heatmap of the raw ratio data (Raw), the same data smoothened with running average (RA) and topological statistics (TS, *P*-value) both with window-size 27 for four neuroblastomas. The rightmost panel (Comb) visualizes the average *P*-value for gain and loss. Chromosomal location is displayed on the left with the location of the centromere marked in red. Figure taken from [15] and used with permission.(For interpretation of the reference to color in this legend, the reader is referred to the web version of this article.)

validation. The cell line SK-N-AS is deleted within 1p36.2-p36.3, which has been investigated by FISH and southern blot analysis [35,36]. The proximal SK-N-AS deletion breakpoint was mapped to between *NPPA* and *PLOD*, while the distal breakpoint is proximal of *CDC2L1*. The deletion detected by our method is bordered by *KIAA0495* and *CTNNBIP1*, which is within the region reported. They are thus in a very good accordance. In addition, we also compared the 17q gain results for four NB cell lines (CHP134, IMR-5, SMS-KCNR, and SK-N-AS) with the results in literature by FISH and Q-PCR [37]. Our results confirmed the gains in 17q for all four cell lines and the loss in 17p in SK-N-AS detected by FISH.

We then analyzed the A-CGH data using this method to detect genome-wide alterations of DNA copy number in our NB samples. We identified DNA copy number alterations that involved the majority of the chromosomes in both primary tumors and cell lines (Fig. 4). We confirmed previously reported genomic changes, including gains of whole chromosome 1, 2, 6, 7, 8, 12, 13, 17, 18 and 22, and losses of 3, 4, 9, 11, and 14; partial gains of 1q, 2p, 11p, 12q and 17q; partial losses of 1p, 3p, 4p, 9p, 11q and 14q [38,39]. The most common changes were losses on chromosome 1p, 4 and 11q; gains on 2p, 7, and 17q [14].

6. Stage specific genomic alterations and evolutionary models of NB progression

We also analyzed the genomic alteration data to explore possible evolutionary models of NB tumor progression. These genomic alterations can be used to identify ‘common’ and ‘differential’ regions in the different tumor groups [14]. The term ‘differential’ in this context denotes differences between two groups of tumors with respect to the *frequency*, with which specific regions are altered, as well as systematic differences in the number of DNA copies. In our analysis, we partitioned the tumors into three subgroups for three different stages of NB (stage 1, stage 4 *MYCN*-not-amplified (4−) and amplified (4+)) and found the alterations that were common to all three subgroups, which included gain of 7q32, 17q21, 17q23-24 and loss of 3p21. We also found genomic imbalances that were specific for each of

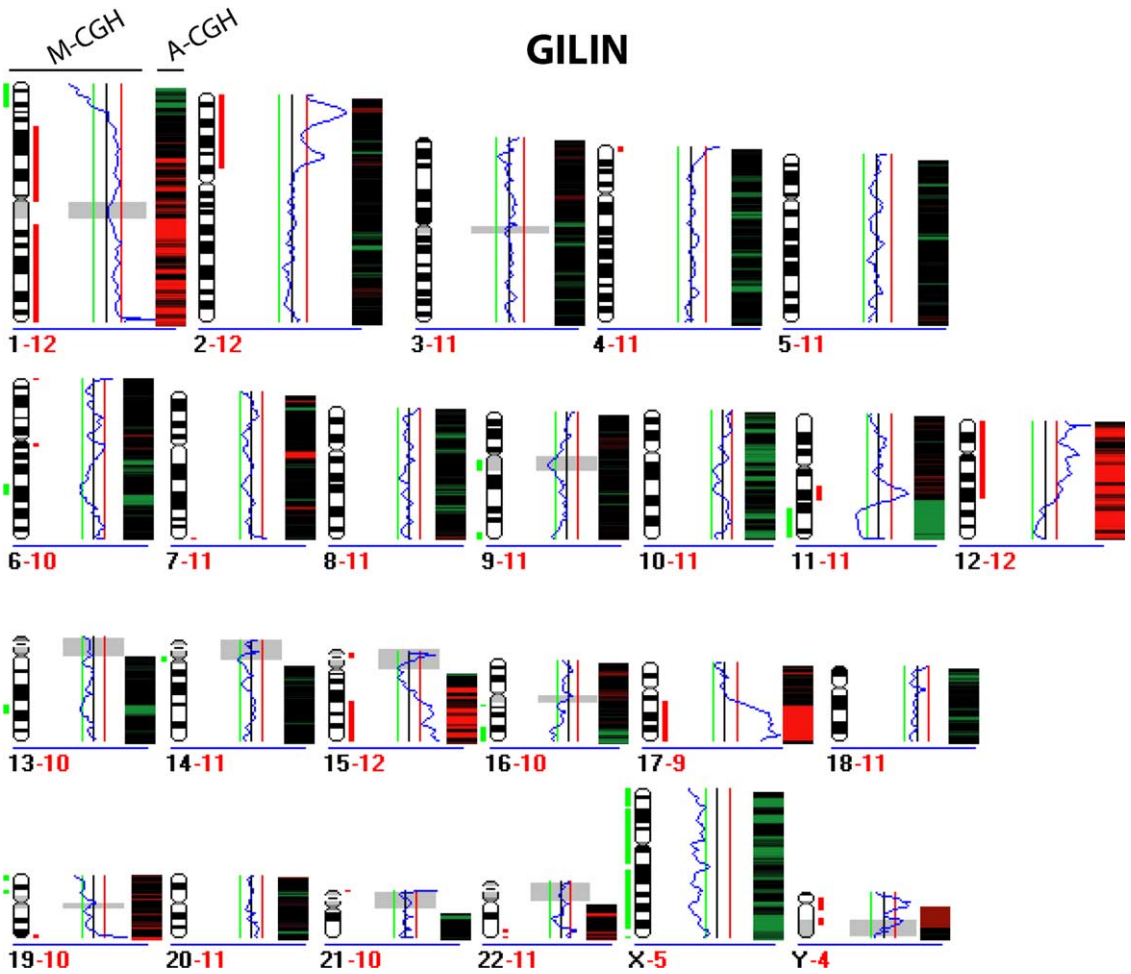

Fig. 3. Chromosomal gains and losses in NB cell line GILIN detected by M-CGH and A-CGH. For M-CGH result, gains are shown as red lines to the right of chromosome and losses as green lines on the left. M-CGH ratio (tumor/reference) is represented as blue curve. Green, black and red lines represent the ratio of 0.8, 1.0, and 1.2, respectively. A-CGH result is represented as the probability heat-map on the right for each chromosome (red for gain and green for loss). (For interpretation of the reference to color in this legend, the reader is referred to the web version of this article.)

the subgroups and common regions of gain for stage 1 and 4− tumors [14]. The presence of these characteristic patterns of genomic alterations suggested that the patterns could be used to derive a phylogeny of different stages of the disease [28,40,41]. By combining genomic information with the stage information we analyzed the possible models of tumor progression. We found that only 10 topologically distinct models of tumor progression exist for a three stage disease based on the three following principles of genetic evolution (Fig. 5A): (1) all tumor stages belonging to the same diagnostic group arise from a common ancestor (i.e. are dealing with a rooted tree). (2) All changes within a parent genotype must be present in the daughter occurring with a similar frequency (the inheritance signature). The daughter will acquire additional genomic changes. (3) The unobserved intermediate genotypes are possible but the model with the smallest number of genotypes (observed+unobserved) is utilized (Occam's Razor [42]). By fitting the models to our observed genomic alterations [14] in each subgroup without

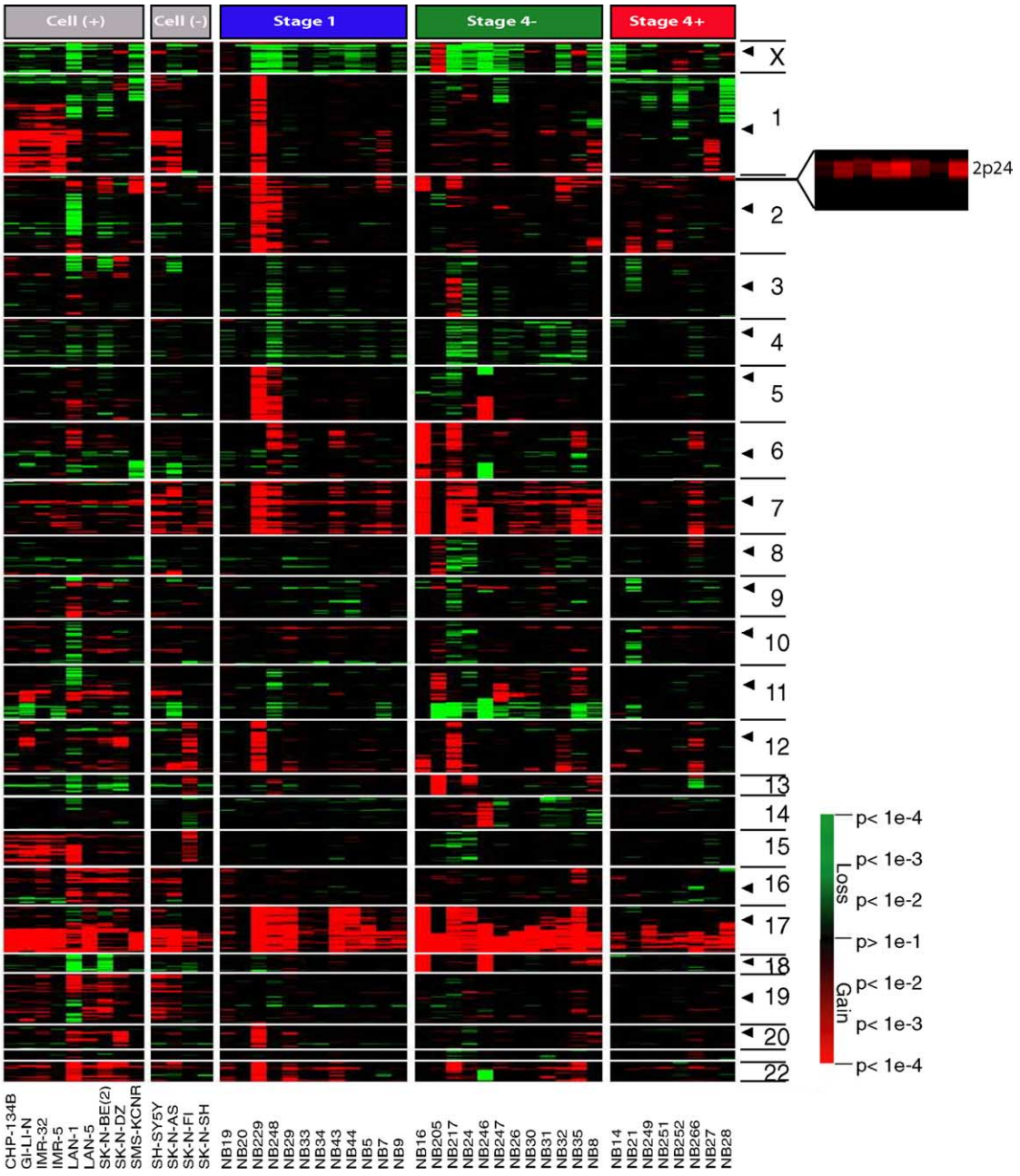

Fig. 4. Genome-wide analysis of DNA copy number alteration by A-CGH. Samples were grouped based on sample type, *MYCN* amplification status and tumor stage. Each column represents a different sample; and each row represents a *P*-value of a given SWlocus using a sliding window of 40 adjacent clones, ordered in genome order across the whole genome. Black triangles on the right side of image represent centromere positions. Cell−, cell line without *MYCN* amplification; Cell+, cell line with *MYCN* amplification; Stage 4−, tumor in stage 4 without *MYCN* amplification; Stage 4+, tumor in stage 4 with *MYCN* amplification. On the right is shown an enlarged view of the region around the *MYCN* gene (2p24) for the amplified NB samples. Figure taken from [14] and used with permission.(For interpretation of the reference to color in this legend, the reader is referred to the web version of this article.)

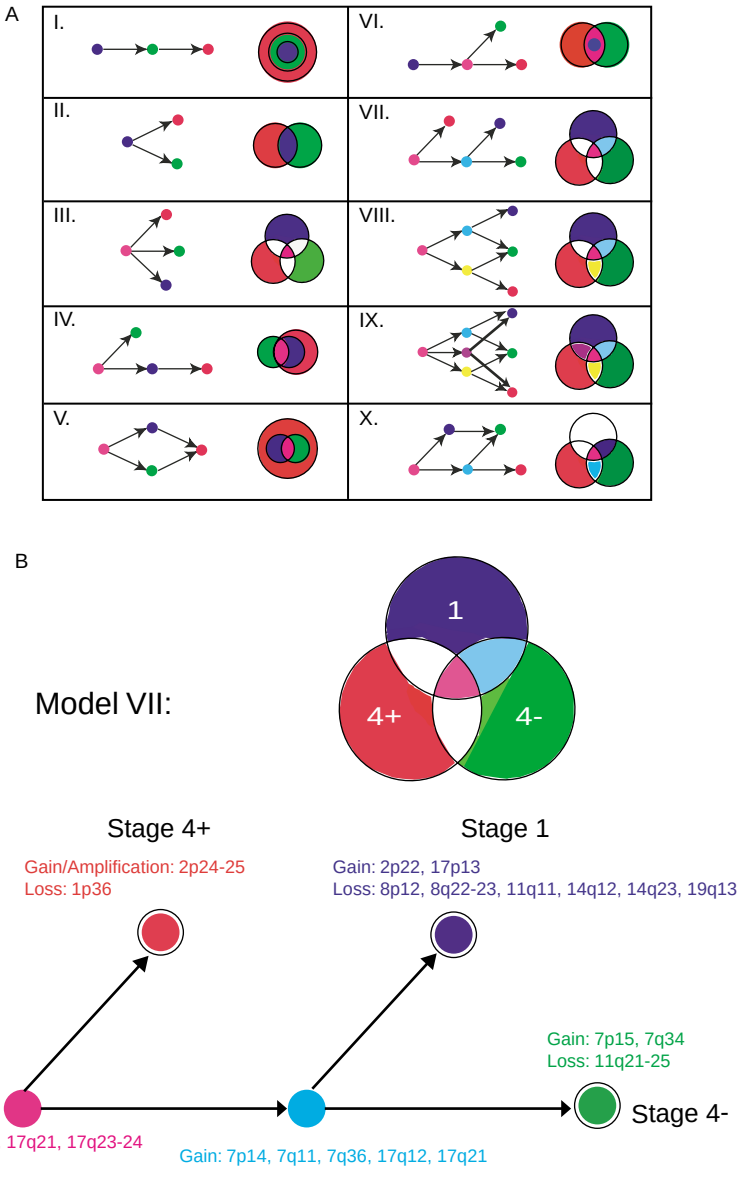

Fig. 5. Hypothetical genetic evolution models in neuroblastoma. (A) All possible genetic evolution models given three subgroups or phenotypes (red, blue and green), cyan and magenta represent intermediate features that are common to two and three groups. Arrow delineates direction of progression. The Venn diagrams next to the tree models show the expected differential and common genomic changes found in each of the phenotypes. For instance in model I: the blue phenotype (e.g. Stage 1) progresses to green or red (e.g. Stage 4− or 4+), such that in the Venn diagram all genomic imbalances present in the 'blue' tumors should also be present in the 'green' and 'red' tumors, whereas the 'red' one includes the extra mutations of the 'green' tumors and its own specific mutations. (B) The best fitting hypothetical gene evolution model in neuroblastoma for our data is model VII. End nodes colored in blue and green and red represent specific mutations present in stage 1, 4− and 4+, respectively. Magenta node represents the common features for all tumors (1, 4−, and 4+), i.e. all mutations in magenta are present in all different stages of tumors (1, 4− and 4+). Cyan node represents the common features for 1 and 4−, i.e. all mutations in cyan exist in stage 1 and 4−. Besides the common features, stage 1, 4−, and 4+ tumors acquire their own specific mutations labeled in blue, green and red, respectively.(For interpretation of the reference to color in this legend, the reader is referred to the web version of this article.)

contradictions to the three principles, we found that only model VII is qualified and can explain our genetic evolution hypothesis (Fig. 5B). In this tree model, three end nodes represent three different subgroups (stage 1, stage 4−, and stage 4+); two intermediate nodes are introduced to represent the common genomic features in two or more groups; arrows represent accumulation of genomic alteration. Tumorigenesis and progression is thought to be a multi-step process in which genetic alteration accumulates sequentially, ultimately producing the neoplastic phenotype [43]. Unlike the simple linear progression model, where the stages are ordered according to the aggressiveness of the disease and the tumor develops from a localized stage 1 tumor to a metastatic stage 4− to 4+ tumor, our data suggest a more complicated genetic evolution pattern in NB. It indicates that NB of stage 1−, stage 4− and stage 4+ do not evolve sequentially, stage 4+ tumors are not derived from stage 1 and stage 4− and they represent different subgroups with different genetic features, which is also supported by the previous clinical evidence [44]. Therefore, the data suggests a hypothetical model, where the final stage of NB is predetermined at the time they acquire specific genomic changes. The first intermediate node, proposed by our model, may represent the genomic changes found in the 'neuroblastic nodules', which resemble 'neuroblastoma in situ' that commonly occurs as incidental findings in infants younger than 3 months who die of other causes [45]. These neuroblastic nodules would ordinarily regress during normal development, however, would undergo malignant transformation if additional hits occur such as loss of 1p36 and *MYCN* amplification which would lead to stage 4+, or other changes that lead to stages 1 or 4− as described. Remarkably stage 4+ disease appears to have very few genomic alterations when compared with stage 1 and 4− implying that *MYCN* amplification is sufficient to drive these tumors to an aggressive phenotype, and although other genomic changes occur, including loss of 1p36 as shown by us and others [46], it does not require extensive changes. This is in agreement with the murine *MYCN* transgenic model of NB where the *MYCN* transgene itself is enough for tumor development, but these tumors develop additional genomic changes characteristic of NB [47].

A different hypothetic model of genetic origin of neuroblastoma was previously proposed based on the expression of two genes *TRKA* and *TRKB* [48–50], and suggesting that there are at least three distinct types of neuroblastoma. Type 1 tumors are characterized by high *TRKA* expression and seem to have a fundamental defect in mitotic disjunction. They are hyperdiploid due to whole chromosome gains and structural rearrangements are rarely observed. Patients with type I tumors are usually cured with surgery alone [49]. On the other hand, tumors that predominantly express *TRKB* are characterized by genomic instability. Structural rearrangements occur and unbalanced 17q gain occurs in most. Tumors that also acquire loss of genetic information on the long arms of chromosomes 11 and/or 14 rarely have 1p loss or *MYCN* amplification (type 2). However, tumors that acquire 1p loss often also acquire *MYCN* amplification and a highly malignant clinical behavior (type 3) and such patients have a poor survival probability of less than 25% [49].

The finding of stage and prognosis specific genomic alterations in NB allows for the development of both of the hypothetical tumor progression models outlined above. However, larger studies are required to confirm which of these models are valid or whether an alternative progression model exists perhaps based on the combination of these two tumor evolution models.

7. Conclusion

Array-based CGH is a high-throughput technique that allows screening of the whole genome in high resolution. This technique is likely to be used increasingly to identify the genomic alterations that are responsible for malignant transformation and develop tumor progression models in neuroblastoma.

Acknowledgements

We thank A Roschke in Dr IR Kirsch's lab for her help with M-CGH experiment.

References

[1] G.M. Brodeur, Neuroblastoma: biological insights into a clinical enigma, Nat. Rev. Cancer 3 (2003) 203–216.

[2] G.M. Brodeur, C. Azar, M. Brother, J. Hiemstra, B. Kaufman, H. Marshall, et al., Neuroblastoma. Effect of genetic factors on prognosis and treatment, Cancer 70 (1992) 1685–1694.

[3] C. Brinkschmidt, H. Christiansen, H.J. Terpe, R. Simon, W. Boecker, F. Lampert, S. Stoerkel, Comparative genomic hybridization (CGH) analysis of neuroblastomas—an important methodological approach in paediatric tumour pathology, J. Pathol. 181 (1997) 394–400.

[4] D. Plantaz, J. Vandesompele, N. Van Roy, M. Lastowska, N. Bown, V. Combaret, et al., Comparative genomic hybridization (CGH) analysis of stage 4 neuroblastoma reveals high frequency of 11q deletion in tumors lacking MYCN amplification, Int. J. Cancer 91 (2001) 680–686.

[5] N. Cohen, D.R. Betts, L. Trakhtenbrot, F.K. Niggli, N. Amariglio, F. Brok-Simoni, et al., Detection of unidentified chromosome abnormalities in human neuroblastoma by spectral karyotyping (SKY), Genes Chromosomes Cancer 31 (2001) 201–208.

[6] G. Schleiermacher, I. Janoueix-Lerosey, V. Combaret, J. Derre, J. Couturier, A. Aurias, O. Delattre, Combined 24-color karyotyping and comparative genomic hybridization analysis indicates predominant rearrangements of early replicating chromosome regions in neuroblastoma, Cancer Genet. Cytogenet. 141 (2003) 32–42.

[7] A. Kallioniemi, O.P. Kallioniemi, D. Sudar, D. Rutovitz, J.W. Gray, F. Waldman, D. Pinkel, Comparative genomic hybridization for molecular cytogenetic analysis of solid tumors, Science 258 (1992) 818–821.

[8] M. Lastowska, E. Nacheva, A. McGuckin, A. Curtis, C. Grace, A. Pearson, N. Bown, Comparative genomic hybridization study of primary neuroblastoma tumors. United Kingdom Children's Cancer Study Group, Genes Chromosomes Cancer 18 (1997) 162–169.

[9] J. Vandesompele, N. Van Roy, M. Van Gele, G. Laureys, P. Ambros, P. Heimann, et al., Genetic heterogeneity of neuroblastoma studied by comparative genomic hybridisation, Genes Chromosomes Cancer 23 (1998) 141–152.

[10] S. Solinas-Toldo, S. Lampel, S. Stilgenbauer, J. Nickolenko, A. Benner, H. Dohner, et al., Matrix-based comparative genomic hybridization: biochips to screen for genomic imbalances, Genes Chromosomes Cancer 20 (1997) 399–407.

[11] D. Pinkel, R. Segraves, D. Sudar, S. Clark, I. Poole, D. Kowbel, et al., High resolution analysis of DNA copy number variation using comparative genomic hybridization to microarrays, Nat. Genet. 20 (1998) 207–211.

[12] A.M. Snijders, N. Nowak, R. Segraves, S. Blackwood, N. Brown, J. Conroy, et al., Assembly of microarrays for genome-wide measurement of DNA copy number, Nat. Genet. 29 (2001) 263–264.

[13] J.R. Pollack, C.M. Perou, A.A. Alizadeh, M.B. Eisen, A. Pergamenschikov, C.F. Williams, et al., Genomewide analysis of DNA copy-number changes using cDNA microarrays, Nat. Genet. 23 (1999) 41–46.

[14] Q.R. Chen, S. Bilke, J.S. Wei, C.C. Whiteford, N. Cenacchi, A.L. Krasnoselsky, et al., cDNA array-CGH profiling identifies genomic alterations specific to stage and MYCN-amplification in neuroblastoma, BioMed Cent Genomics 5 (2004) 70.

[15] S. Bilke, Q.R. Chen, C.C. Whiteford, J. Khan, Detection of low level genomic alterations by comparative genomic hybridization based on cDNA micro-arrays, Bioinformatics 21 (2005) 1138–1145.

[16] A.S. Ishkanian, C.A. Malloff, S.K. Watson, R.J. DeLeeuw, B. Chi, B.P. Coe, et al., A tiling resolution DNA microarray with complete coverage of the human genome, Nat. Genet. 36 (2004) 299–303.

[17] D.G. Albertson, Profiling breast cancer by array CGH, Breast Cancer Res. Treat. 78 (2003) 289–298.

[18] J.R. Pollack, T. Sorlie, C.M. Perou, C.A. Rees, S.S. Jeffrey, P.E. Lonning, et al., Microarray analysis reveals a major direct role of DNA copy number alteration in the transcriptional program of human breast tumors, Proc. Natl Acad. Sci. USA 99 (2002) 12963–12968.

[19] E. Hyman, P. Kauraniemi, S. Hautaniemi, M. Wolf, S. Mousses, E. Rozenblum, et al., Impact of DNA amplification on gene expression patterns in breast cancer, Cancer Res. 62 (2002) 6240–6245.

[20] C. Brennan, Y. Zhang, C. Leo, B. Feng, C. Cauwels, A.J. Aguirre, et al., High-resolution global profiling of genomic alterations with long oligonucleotide microarray, Cancer Res. 64 (2004) 4744–4748.

[21] B. Carvalho, E. Ouwerkerk, G.A. Meijer, B. Ylstra, High resolution microarray comparative genomic hybridisation analysis using spotted oligonucleotides, J. Clin. Pathol. 57 (2004) 644–646.

[22] G.R. Bignell, J. Huang, J. Greshock, A. Watt, A. Butler, S. West, et al., High-resolution analysis of DNA copy number using oligonucleotide microarrays, Genome Res. 14 (2004) 287–295.

[23] B. Beheshti, I. Braude, P. Marrano, P. Thorner, M. Zielenska, J.A. Squire, Chromosomal localization of DNA amplifications in neuroblastoma tumors using cDNA microarray comparative genomic hybridisation, Neoplasia 5 (2003) 53–62.

[24] K. De Preter, F. Pattyn, G. Berx, K. Strumane, B. Menten, F. Van Roy, et al., Combined subtractive cDNA cloning and array CGH: an efficient approach for identification of overexpressed genes in DNA amplicons, BioMed Cent Genomics 5 (2004) 11.

[25] P.N. Tonin, H. Yeger, R.L. Stallings, P.R. Srinivasan, W.H. Lewis, Amplification of N-myc and ornithine decarboxylase genes in human neuroblastoma and hydroxyurea-resistant hamster cell lines, Oncogene 4 (1989) 1117.

[26] K. De Preter, F. Speleman, V. Combaret, J. Lunec, G. Laureys, B.H. Eussen, et al., Quantification of MYCN, DDX1, and NAG gene copy number in neuroblastoma using a real-time quantitative PCR assay, Mod. Pathol. 15 (2002) 159–166.

[27] H. Kuroda, P.S. White, E.P. Sulman, C.F. Manohar, J.L. Reiter, S.L. Cohn, G.M. Brodeur, Physical mapping of the DDX1 gene to 340 kb 5′ of MYCN, Oncogene 13 (1996) 1561–1565.

[28] T.A. Jones, R.H. Flomen, G. Senger, D. Nizetic, D. Sheer, The homeobox gene MEIS1 is amplified in IMR-32 and highly expressed in other neuroblastoma cell lines, Eur. J. Cancer 36 (2000) 2368–2374.
[29] B.C. Armstrong, G.W. Krystal, Isolation and characterization of complementary DNA for N-cym, a gene encoded by the DNA strand opposite to N-myc, Cell Growth Differ. 3 (1992) 385–390.
[30] K. Wimmer, X.X. Zhu, B.J. Lamb, R. Kuick, P.F. Ambros, H. Kovar, et al., Coamplification of a novel gene, NAG, with the N-myc gene in neuroblastoma, Oncogene 18 (1999) 233–238.
[31] I. Miyake, Y. Hakomori, A. Shinohara, T. Gamou, M. Saito, A. Iwamatsu, R. Sakai, Activation of anaplastic lymphoma kinase is responsible for hyperphosphorylation of ShcC in neuroblastoma cell lines, Oncogene 21 (2002) 5823.
[32] R. Corvi, L. Savelyeva, S. Breit, A. Wenzel, R. Handgretinger, J. Barak, et al., Non-syntenic amplification of MDM2 and MYCN in human neuroblastoma, Oncogene 10 (1995) 1081–1086.
[33] P. Hupe, N. Stransky, J.P. Thiery, F. Radvanyi, E. Barillot, Analysis of array CGH data: from signal ratio to gain and loss of DNA regions, Bioinformatics 20 (2004) 3413–3422.
[34] K. Jong, E. Marchiori, G. Meijer, A. Van Der Vaart, B. Ylstra, Breakpoint identification and smoothing of array comparative genomic hybridization data, Bioinformatics 20 (2004) 3636–3637.
[35] N.C. Cheng, N. Van Roy, A. Chan, M. Beitsma, A. Westerveld, F. Speleman, R. Versteeg, Deletion mapping in neuroblastoma cell lines suggests two distinct tumor suppressor genes in the 1p35-36 region, only one of which is associated with N-myc amplification, Oncogene 10 (1995) 291–297.
[36] P.S. White, J.M. Maris, C. Beltinger, E. Sulman, H.N. Marshall, M. Fujimori, et al., A region of consistent deletion in neuroblastoma maps within human chromosome 1p36.2–36.3, Proc. Natl Acad. Sci. USA 92 (1995) 5520–5524.
[37] M. Morowitz, S. Shusterman, Y. Mosse, G. Hii, C.L. Winter, D. Khazi, et al., Detection of single-copy chromosome 17q gain in human neuroblastomas using real-time quantitative polymerase chain reaction, Mod. Pathol. 16 (2003) 1248–1256.
[38] G.P. Tonini, M. Romani, Genetic and epigenetic alterations in neuroblastoma, Cancer Lett. 197 (2003) 69–73.
[39] J. Vandesompele, F. Speleman, N. Van Roy, G. Laureys, C. Brinskchmidt, H. Christiansen, et al., Multicentre analysis of patterns of DNA gains and losses in 204 neuroblastoma tumors: how many genetic subgroups are there?, Med. Pediatr. Oncol. 36 (2001) 5–10.
[40] A. von Heydebreck, B. Gunawan, L. Fuzesi, Maximum likelihood estimation of oncogenetic tree models, Biostatistics 5 (2004) 545–556.
[41] M.D. Radmacher, R. Simon, R. Desper, R. Taetle, A.A. Schaffer, M.A. Nelson, Graph models of oncogenesis with an application to melanoma, J. Theor. Biol. 212 (2001) 535–548.
[42] T.F. Smith, Occam's razor, Nature 285 (1980) 620.
[43] E.R. Fearon, B. Vogelstein, A genetic model for colorectal tumorigenesis, Cell 61 (1990) 759–767.
[44] F. Westermann, M. Schwab, Genetic parameters of neuroblastomas, Cancer Lett. 184 (2002) 127–147.
[45] J. Beckwith, E. Perrin, In situ neuroblastomas: a contribution to the natural history of neural crest tumors, Am. J. Pathol. 43 (1963) 1089–1104.
[46] C.T. Fong, N.C. Dracopoli, P.S. White, P.T. Merrill, R.C. Griffith, D.E. Housman, G.M. Brodeur, Loss of heterozygosity for the short arm of chromosome 1 in human neuroblastomas: correlation with N-myc amplification, Proc. Natl Acad. Sci. USA 86 (1989) 3753–3757.
[47] C.S. Hackett, J.G. Hodgson, M.E. Law, J. Fridlyand, K. Osoegawa, P.J. De Jong, et al., Genome-wide array CGH analysis of murine neuroblastoma reveals distinct genomic aberrations which parallel those in human tumors, Cancer Res. 63 (2003) 5266–5273.
[48] G.M. Brodeur, J.M. Maris, D.J. Yamashiro, M.D. Hogarty, P.S. White, Biology and genetics of human neuroblastomas, J. Pediatr. Hematol. Oncol. 19 (1997) 93–101.
[49] J. Maris, K.K. Matthay, Molecular biology of neuroblastoma, J. Clin. Oncol. 17 (1999) 2264–2279.
[50] I.M. Ambros, G.M. Brodeur, Concept of tumorigenesis and regression in: G.M. Brodeur, T. Sawada, Y. Tsuchida, P.A. Voute (Eds.), Neuroblastoma, Elsevier Science B.V., Amsterdam, 2000, pp. 21–32.